Growth of vertically aligned carbon nanotubes for electrical applications using water-assisted chemical vapor deposition

Author: Irene Iglesias Vallez.
Faculty of Physics, Universitat de Barcelona, Diagonal 645, 08028 Barcelona, Spain.*

Abstract: Vertically aligned carbon nanotubes (VACNTs) were successfully grown by water-assisted chemical vapor deposition (WACVD) on different substrates. Using water and acetylene, we were able to produce samples of dense and aligned carbon nanotubes (CNTs), and remove the amorphous carbon generated during synthesis.

The CNTs samples were grown on silicon, copper, graphite and carbon paper substrates, using different thin films as diffusion barriers between catalyst and substrate materials. Silicon was chosen because of the number of published studies regarding synthesis on this substrate and due to its widespread use in electronics and microelectronics. Nanotubes were also grown on conductor substrates such as Cu, carbon paper or graphite because of their interesting electrical applications, such as the widespread use of copper for electrodes.

The CNTs obtained were highly vertically aligned, dense and ordered, as characterized by scanning electron microscopy, and of considerable length (ranging from 20 to 200 μm). VACNTs were obtained on all substrates used. The electrochemical behavior of CNTs grown on carbon paper and graphite was characterized by cyclic voltammetry, showing promising electrical properties, such as 90 $mF \cdot cm^{-2}$ area capacitance, to yield high quality devices. Raman spectroscopy was used to characterize their morphological structure and prove the existence of single-wall nanotubes.

I. INTRODUCTION

Since their modern rediscovery, due to the work of Iijima in 1991 [1], carbon nanotubes have been actively studied. They are being investigated in an attempt to harness their unique electronic, optical and mechanical properties. They have been used for specific and promising novel applications, such as supercapacitors, electron-emission sources, hydrogen storage materials, a wide range of sensors and electronics on flexible substrates, to name a few [1, 2, 3].

Their inherently one-dimensional nature, which is reflected in their density of states (Van Hove singularities), gives them unique properties, such as the ballistic transport of charges, large quantum oscillations or quantum capacitance that is not seen in bulky materials [1]. For example they possess a current capacity that is 1000 times higher than that of copper wires.

Nanotubes are 10,000 times thinner than human hair, have a Young's modulus of around 1 TPa, possess a high tensile strength and are up to 100 times stronger than steel [1, 2].

Fundamentally, CNTs can be understood as a folding or wrapping of a graphene sheet. There are an infinite number of ways to roll a sheet into a cylinder, resulting in different diameters and microscopic structures of the tubes. These different configurations of CNTs are described by the chirality concept, which refers to how the tubes are coiled about axis T in the plane of graphite. This is the only unique characteristic of a nanotube that determines its exact diameter and enables the most accurate computation of all its solid-state properties [2].

Nanotubes are classified according to the symmetry of their physical structure, resulting in armchair, zigzag and chiral nanotubes, with armchair and zigzag types exhibiting a higher symmetry than chiral nanotubes [2].

Electronically, CNTs can be either metallic or semiconducting depending on diameter and chirality, and this diversity makes CNTs very attractive for a wide variety of applications. In general, armchair CNTs are metallic, zig-zag CNTs are semiconducting and chiral CNTs are mostly semiconducting, except when their chirality is an integer multiple of three, when they are metallic [1, 2].

There are two groups of CNTs, single-wall (SWCNTs) and multi-wall carbon nanotubes (MWCNTs). SWCNTs are hollow cylindrical or more precisely polyhedral, structures of carbon atoms, with lengths in the order of micrometers and a diameter that ranges from about 0.5 to 5 nm. Although, similar in structure to single-wall CNTs, MWCNTs have multiple nested or concentric cylindrical walls, with a space between walls of approximately 0.34 nm, comparable to the interlayer spacing in graphite. Both have similar lengths, but MWCNTs are of much larger diameter. Their inner and outer diameters are around 5 and 100 nm respectively, corresponding to ≈ 30 coaxial tubes. Confinement effects are expected to be less dominant than in single-walled tubes, because of the large circumference [1, 2].

There are three different ways of synthesizing carbon nanotubes; arc discharge, laser ablation and chemical vapor deposition (CVD).

The arc discharge technique has two major disadvantages, the low control on; the diameter and the alignment of CNTs. Furthermore, it often generates a variety of carbon structures, simultaneously produced alongside nanotubes, and the product has to be subsequently separated and processed for greater purity [1-3].

Laser ablation is a very well known technique for the production of CNTs. It offers control over the deposition parameters, allowing good control over the final characteristics of CNTs, enabling the production of high crystalline CNTs. Nevertheless, it has the same problem as arc discharge, requiring subsequent processing of the product.

Finally, growth by CVD is the technique that offers most possibilities for applications of this material, due to the possibility of growing CNT on multiple substrates and geometries [2, 3]. Additionally, it allows better control of certain characteristics of the CNTs, such as alignment, average diameter and length.

At present, some forms of post-synthetic treatment of CNTs are required to sort nanotubes, so as to achieve a

* Electronic address: iiglesiasvallez@gmail.com

narrower distribution with more uniform properties, because all synthesis methods result in a variety of nanotubes with a distribution in diameter [2, 3].

In this work, the objective was to synthesize VACNTs which present several advantages with respect to non-aligned ones; highly conductive, low contact resistance, large specific surface area and fast electron transfer kinetics [2, 4, 5].

There are two variants of the CVD technique, Plasma-Enhanced chemical vapor deposition (PECVD) and WA-CVD used to grow VACNT. In our case, we used the last one, resulting in denser nanotube samples than PECVD. Water vapor acts in promoting and preserving catalytic activity by removing amorphous carbon during the synthesis. As a result, the efficiency of the synthesis can be increased, resulting in the formation of densely packed, defect-free, VACNT forests [6-8].

II. EXPERIMENTAL

A. Substrates preparation

The different samples were composed of a substrate with a diffusion barrier of alumina (Al_2O_3) on top, before the iron catalyst layer. Alumina was used as a diffusion barrier, to stop catalytic particles diffusing through the substrate and thus allowing successful annealing and catalyst particle formation. Alumina also increases CNT adhesion to the substrate and dissociation of carbon source during the synthesis process. Only 30 nm was deposited, so as not to act as insulation and affect conduction [9, 10]. Two of the cooper samples (C and D) also contained Ni and/or Ti layers between substrate and alumina, to improve adhesion. These intermediate layers have been used to eliminate cracking of the cooper surface during the synthesis of CNTs, in order to improve CNT adhesion on Cu substrate [3, 9].

Before the VACANTs synthesis process, thin layer deposition of different materials was carried out on a plasma enhanced deposition reactor. The description of each sample, the substrate used, the deposited material and the thickness of the layers appear in order from substrate to alumina in Table I.

Sample	**A**	**B**	**C**	**D**	**E**	**F**
Substrate	Si	Cu	Cu	Cu	Graphite	Carbon paper
Diffusion barrier						
Ni (nm)	-	56	-	-	-	-
Ti (nm)	-	75	75	-	-	-
Al_2O_3(nm)	30	30	30	30	30	30

TABLE I: Description of the substrates and thickness of the different deposited layers used for each sample.

Three different diffusion barriers were deposited under different conditions. The first two were deposited by means of Pulsed DC magnetron sputtering, using Ni and Ti targets. The argon sputtering pressure was 1 Pa with 20 sccm gas flow. Plasma was carried out at a pulsed frequency of 100 kHz, pulse width 2016 ns and different pulsed powers depending on the sample, as shown in Table II. The sample was kept at room temperature. The sputtering plasma was powered by a DC source working in current regulation mode.

Target	Ni	Ti	Al	Al_2O_3
Power pulsed (W)	120	50	90	120

TABLE II: Power used during sputtering of each material.

The top layer, alumina (Al_2O_3), was deposited through reactive magnetron sputtering, using Al target and a gas mixture of Ar (34 sccm) and O_2 (6 sccm). With the same conditions described above. Before starting Al deposition, it was cleaned with argon plasma (1 Pa, 20 sccm, 120 W) during 10 minutes.

B. Synthesis Reactor for VACNTs growth

The growth of VACNTs was carried out in a WACVD reactor, Fig. (1). The reactor incorporates three magnetron sputtering heads, one of which (Fe) was used for the catalyst thin layer deposition.

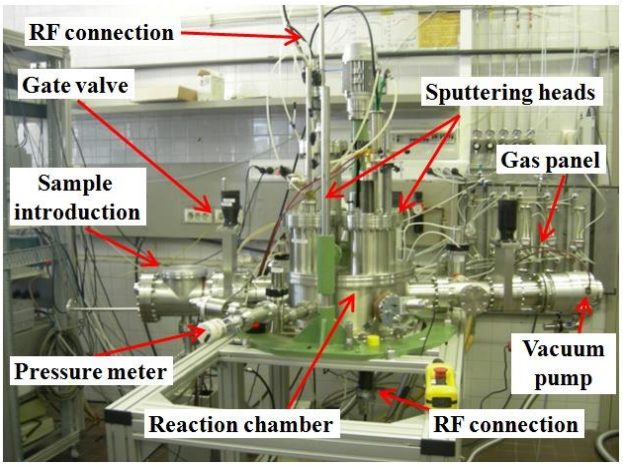

FIG. 1: Carbon nanotubes growth reactor.

After 2 nm iron deposition, annealing of catalyst thin film was carried out at a temperature of up to 600 ºC, with a ramp time of 750 s in a reducing atmosphere of hydrogen (100 sccm) at a pressure of 2 mbar. Catalyst nanoislands were allowed to form for 2 minutes at 600 ºC (hold time). After hold time, the pressure inside the reactor was lowered to 1 mbar and C_2H_2 (50 sccm) was introduced into the chamber. Then the temperature was rapidly increased over the next 10 s, up to 700 ºC. The water flask outlet was opened ~15 s after the introduction of C_2H_2 (0.04 sccm water flow). Growth time was 15' in all samples, except in sample E (20').

III. RESULTS AND DISCUSSION

A. Scanning Electron Microscopy (SEM)

Surface morphology (length, homogeneity and adhesion on substrates) characterization of VACNTs was carried out by Scanning Electron Microscopy (SEM) studies using a SEM Joel J-6510 microscope. Figure (2) shows the SEM images of samples A, F and C. These were chosen because they are the most significant to observe the clear differences in morphology, related to the type of substrate used. A flat substrate, such as silicon, a fibrous substrate, carbon paper and a metallic substrate, copper, lead to different surfaces. In these images the high quality, density and alignment of the VACNTs can be clearly seen.

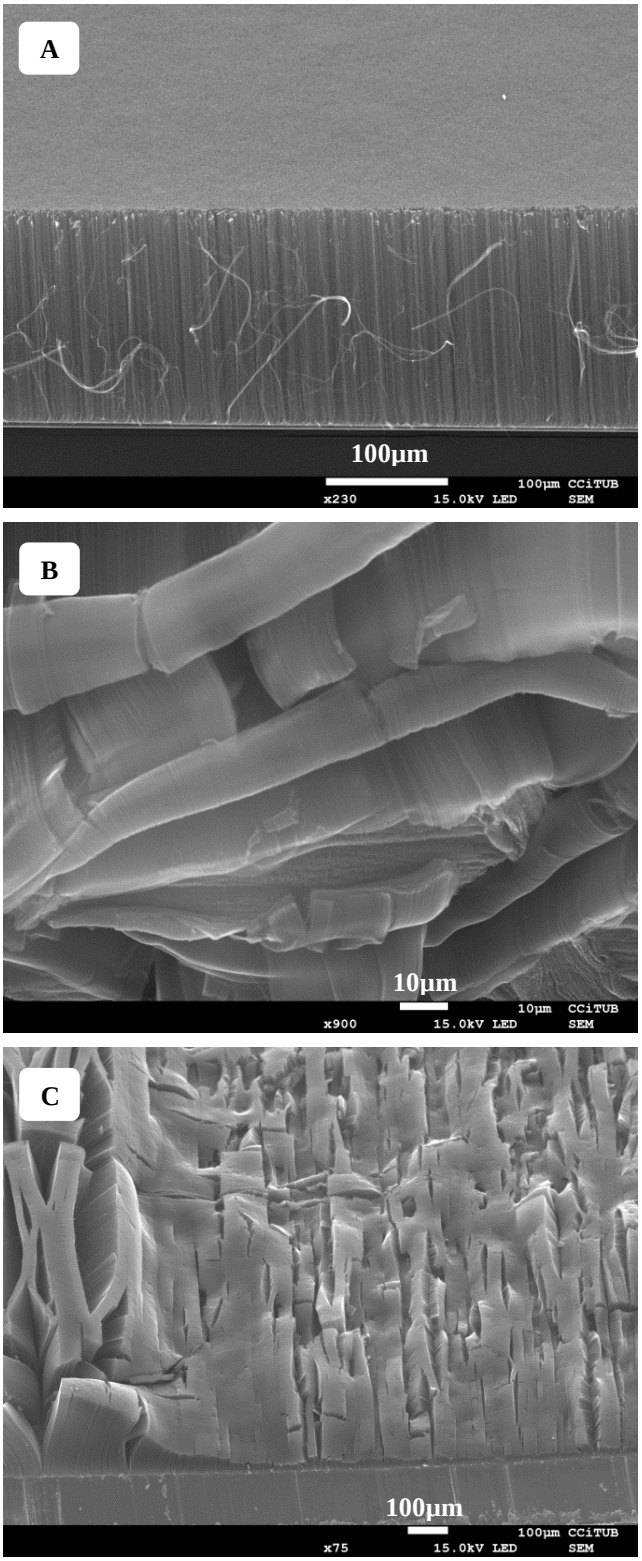

FIG. 2: SEM images of vertically aligned carbon nanotubes grown using WACVD. (a**)** Sample A, (b) Sample F, (c) Sample C.

Figure (2a) shows VACNTs grown on silicon. The nanotubes obtained on this substrate were of high density and homogeneous in height. Very long nanotubes of approximately 180 µm were able to be grown and these remained perfectly vertically aligned.

Figure (2b) shows VACNTs grown on carbon paper. This sample is densely covered in nanotubes that have grown in vertical alignment to the substrate. As the substrate is composed of interlaced fibers, the nanotubes have grown in all directions, completely covering each fiber, and are of differing lengths, ranging from 25 to 150 µm. The variety of lengths can be explained by different thicknesses of the catalyst and diffuse layers, caused by the relief of such a fibrous surface. In this sample, the upper parts of the nanotubes are curved, due to their own weight and the fact that they have no nearby neighbors of similar length.

Figure (2c) shows that vertically aligned nanotubes can be successfully grown on a Cu substrate. This is a remarkable finding, due to the relatively small number of published studies on their growth on Cu and its extensive use in electrodes. The nanotubes in this sample are 20 µm in length at their shortest (the right hand side of the image), whilst at their longest (on the left) they reach 200 µm in length. This difference in height was eliminated in sample B, which was similar to sample C, but with a layer of Ni between the Cu substrate and the Ti coating. Here, a nanotube height of 15 µm was obtained across the sample. Further studies should be undertaken using a variety of different thicknesses of Ti and Ni layers to establish the optimum length, homogeneity and adherence of the nanotubes.

B. Raman

Carbon nanotubes samples were examined using micro-Raman spectroscopy (HORIVA LabRam HR800, Japan). During measurement we used a green 0.5 mW laser of 532 nm wavelength and a long working distance (LWD) objective, with a beam spot of 0.7µm.

Raman spectroscopy is one of the most powerful techniques CNTs characterization. A non-destructive technique, it offers non-contact measurement, providing a wealth of information without needing sample preparation [11].

In Raman spectra, Fig. (3), two characteristic bands of CNTs, the D-band and the G-band can be seen [11]. The presence of these bands confirm that CNTs have grown in our samples.

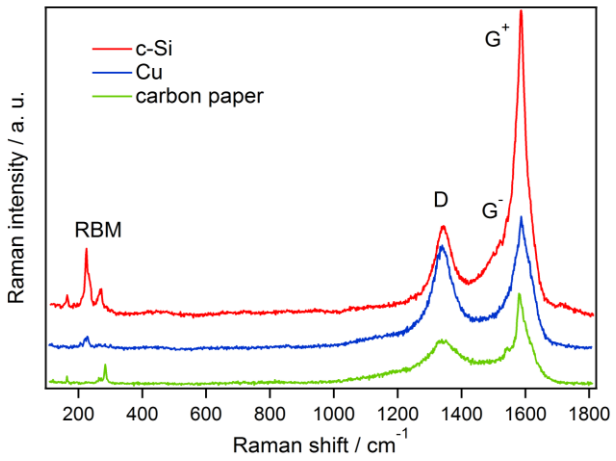

FIG. 3: Raman spectra of carbon nanotubes grown on sample A (c-Si), sample B (Cu) and sample F (carbon paper).

The D-band (1330-1360 cm^{-1}), a double resonance Raman mode, indicates the structural disorder coming from amorphous carbon and other defects.

The G-band (1500-1600 cm^{-1}), especially G^-, shows the presence of single wall nanotubes in our sample. We know that because the G-band, a tangential stretching

mode, appears divided into G^+ and G^-, and G^- only appears in the spectra of single wall nanotubes.

Finally, to be sure that the CNTs are single wall, we can examine the radial breathing mode (RBM, 200-400 cm^{-1}). In this mode, atoms around the circumference of a SWCNT vibrate in a radial pattern. These vibration modes, figure 3, characteristic of single-wall CNTs, confirm their existence. These first order Raman features distinguish a SWCNT from all other sp^2 carbon nanostructures [11].

	D band		G band		
Sample	Position (cm^{-1})	Intensity (a.u.)	Position (cm^{-1})	Intensity (a.u.)	**$R = I_D/I_G$**
A	1340.2	12.65	1584.7	38.71	0.32
Error ±	0.4	0.13	0.2	1.66	0.01
B	1342.8	14.90	1589.6	17.40	0.86
Error ±	0.2	0.16	0.4	0.38	0.02
F	1344.0	5.96	1582.2	9.51	0.63
Error ±	0.7	0.22	0.2	0.32	0.03

TABLE III: Position and intensity of D-band and G-band peaks from samples A, B and F, also showing the intensity ratio between D and G modes.

Table III shows the D and G band position from samples A, B and F and their intensities in arbitrary units, useful to calculate the intensity ratio. The intensity ratio ($R = I_D/I_G$) of the disorder induced, D-bans, to the symmetry-allowed, G-band, provides a sensitive measurement system to characterize the defect density in sp^2 carbon materials.

As the ratio decreases, so does the number of structural defects present in the CNTs. Sample A, grown on a silicon wafer, presents the minor ratio ($R = 0.32 \pm 0.01$), revealing fewer structural defects and Sample B, grown on Cu, the maximum ($R = 0.86 \pm 0.02$), showing more structural defects.

C. Electrochemistry

The electrochemical properties of VACNTs grown on graphite and carbon paper (sample E and F), were measured by cyclic voltammetry (CV). A 0.1 M and 1 M Na_2SO_4 aqueous solution were used to analyze the charge storage capability of VACNTs electrodes. The geometrical area of the working electrode was set to a constant value of 0.57 cm^2. All experiments were carried out in a typical three-electrode cell at 25 ºC. An Ag/AgCl electrode (3 M, KCl internal solution) and Pt-ring electrodes were used as the reference and counter electrode, respectively.

The specific area capacitance of VACNTs samples was calculated from CV measurements using the following equation:

$$C_{sa} = \frac{q_a + |q_c|}{2A\Delta V}$$

where C_{sa} is the specific area capacitance in $F \cdot cm^{-2}$, q_a and q_c the anodic and cathodic charge, respectively, in C, A the area of the electrode active surface area in cm^2 and ΔV the voltage in V.

Figure 4 shows the results of the electrochemical analyses of samples E and F. The first three graphs show cyclic voltammograms of VACNTs at different scan rates.

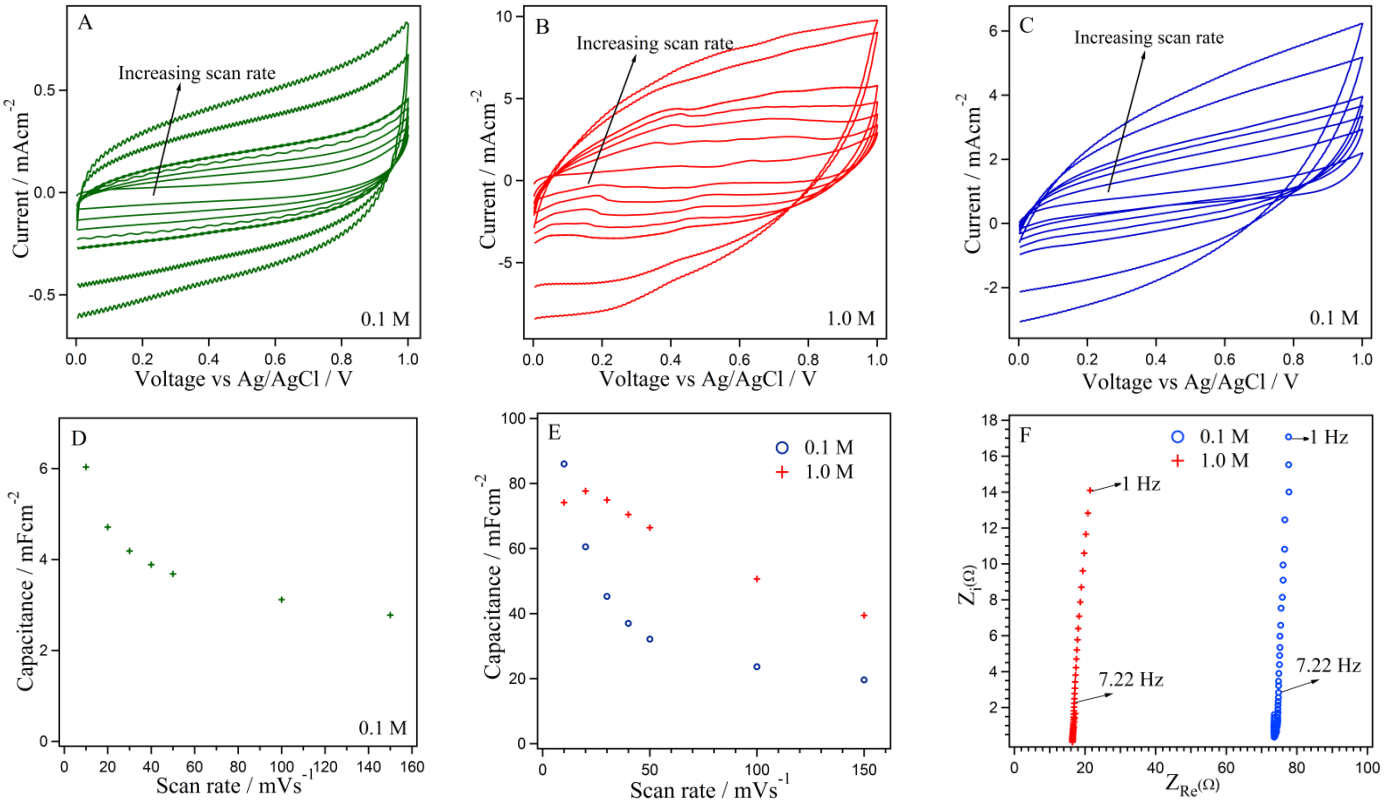

FIG. 4: Graphs of the electrochemical results of VACNTs on graphite (shown in green) and carbon paper (shown in red and blue) substrates. (a) Sample E. Cyclic voltammograms of VACNT electrode at several scan rates (from 10 $mV \cdot s^{-1}$ to 150 $mV \cdot s^{-1}$) in 0.1 M Na_2SO_4 solution. (b) and (c) Sample F. Cyclic voltammograms of VACNT electrode at several scan rates (from 10 $mV \cdot s^{-1}$ to 150 $mV \cdot s^{-1}$), in 0.1 M and 1 M Na_2SO_4 solution, respectively. (d) Sample E (graphite) and (e) Sample F (carbon paper). Specific area capacitance versus scan rate of VACNT electrode. (f) Sample F. Electrochemical impedance spectroscopy. Frequency ranges from 100 kHz to 1Hz.

The scan rate values are 10, 20, 30, 40, 50, 100 and 150 $mV \cdot s^{-1}$. The first graph corresponds to the graphite sample, measured with a 0.1 M electrolyte concentration. VACNTs grown on this substrate present voltammograms typical rectangular-shape with double layer capacitance associated, Fig. (4a) [12, 13]. The second and third graphs are from the carbon paper sample, with 0.1 M and 1 M concentrations, respectively, Fig. (4b) and (4c). These voltammograms show a slight deviation from the rectangular shape, related to pseudocapacitive (faradaic) processes [12, 13].

Even though graphite voltammograms-shape are more rectangular than carbon paper, the specific area capacitance of nanotubes grown on carbon paper (80 $mF \cdot cm^{-2}$ at 10 $mV \cdot s^{-1}$) is more than one order of magnitude higher than those grown on graphite (6 $mF \cdot cm^{-2}$ at 10 $mV \cdot s^{-1}$). These specific area capacitances for different scan rates are shown in figures (4d) and (4e). It can be seen from the graph that capacitance decreases as scan rate increases and increases with electrolyte concentration. It also shows that very good capacitance values were obtained from the samples analyzed [14].

On carbon paper, a maximum capacitance of about 80 $mF \cdot cm^{-2}$ for 1 M and0.1 M Na_2SO_4 aqueous concentration, was achieved, demonstrating good electrical qualities [14], as it was expected, Fig. 4e. The difference in capacitance values is due to the different concentration of electrolyte used in the measurement (0.1 M and 1 M respectively). It indicates an increase of capacitance by increasing the concentration of Na_2SO_4, because, conductivity increases with increasing Na^{2+} ions concentration. This effect was also seen in the voltammograms, where a higher concentration meant a higher current.

A ~6 $mF \cdot cm^{-2}$ capacitance was obtained from the 0.1 M Na_2SO_4 aqueous solution for the graphite sample. Although being a good result, carbon paper sample produced higher capacitances.

Electrochemical impedance spectroscopy (EIS) was performed to analyze the electrodes' kinetic behavior. Figure (4f) demonstrates the Nyquist plot of CNTs/carbon paper for 0.1 and 1 M concentrations of the Na_2SO_4 solution. It can clearly be seen that the electrolyte concentration has a greater effect on impedance. EIS decreases from 73 to 16 Ω with concentration increase.

IV. CONCLUSIONS

- Single-walled, VACNTs were successfully grown on silicon, copper, carbon paper and graphite, from C_2H_2, by WACVD. Lengths ranged from 20 to 200 μm.

- In this paper, we show that high quality VACNTs can be grown on conducting substrates, as Cu or graphite. This is of particular importance in the case of Cu, due to the wide range of electrical applications this offers.

- Good electrical properties were recorded by electrochemical analysis from samples grown on graphite and carbon paper substrates, with maximum capacitances of 80 $mF \cdot cm^{-2}$ and 6 $mF \cdot cm^{-2}$ being reached, respectively. These results show VACNTs grown by WACVD as a good candidate for electrical applications.

Acknowledgements

The author would like to thank Dra. Esther Pascual, Dr. Roger Amade and Mr. Shahzad Hussain for their help and guidance throughout the work. Also she would like to give thanks to FEMAN research group for the reactors and electrochemical system use and to *Centres Científics i Tecnològics* of *Universitat de Barcelona* (CCiTUB) for the use of SEM and RAMAN facilities.

[1] S. Reich, C. Thomsen, and J. Maultzsch, Carbon Nanotubes, 1st. ed. Weinheim: Wiley-VCH, 2004.

[2] P. Wong, and D. Akinwande, Carbon Nanotube and Graphene Device Physics, 1st. ed. New York: Cambridge University Press, 2011.

[3] J. Garcia. "Nanotubos de carbono: síntesis, caracterización y aplicaciones". Ph.D. thesis, Universitat de Barcelona, Barcelona, Spain, 2008.

[4] K. Liu, Y. Sun, L. Chen, C. Feng, X. Feng, K. Jiang, et al. "Controlled growth of super-aligned carbon nanotube arrays for spinning continuous unidirectional sheets with tunable physical properties," Nano Lett, vol. 8, no. 2, pp. 700-705, February 2008.

[5] R. Amade, E. Jover, B. Caglar, T. Mutlu, and E. Bertran, "Optimization of MnO_2/vertically aligned carbon nanotube composite for supercapacitor application," J Power Sourc, vol. 196, pp. 5779-5783, February 2011.

[6] K. Xie, M. Muhler, and W. Xia, "Influence of water on the initial growth rate of carbon nanotubes from ethylene over a cobalt-based catalyst," Ind Eng Chem Res, vol. 52, no. 39, pp. 14.081-14.088, 2013.

[7] S. P. Patole, P. S. Alegaonkar, H.-C. Lee, and J.-B. Yoo, "Optimization of water assisted chemical vapor deposition parameters for super growth of carbon nanotubes," Carbon, vol. 46, pp. 1987-1993, August 2008.

[8] K. Hata, N. Futaba, K. Mizuno, T. Namai, M. Yumura, and S. Iijima, "Water-assisted highly efficient synthesis of impurity-free single-walled carbon nanotubes," Science, vol. 306, pp. 1362-1364, November 2004.

[9] G. Li, S. Chakrabarti, M. Schulz, and V. Shanov, "Growth of aligned multiwalled carbon nanotubes on bulk copper substrates by chemical vapor deposition," J Mater Res, vol. 24, no. 9, pp. 2813-2820, September 2009.

[10] M. Xinhui, C. Bingchu, W. Maosong, and C. Guoping, "Deposition of aluminium oxide films by pulsed reactive sputtering," J Mater Sci Technol, vol. 19, no. 4, pp. 368-370, 2003.

[11] R. Saito, M. Hofmann, G. Dresselhaus, A. Jorio and M. S. Dresselhaus, "Raman spectroscopy of graphene and carbon nanotubes," Adv Phys, vol. 60, no. 3, pp.413-550, 2011.

[12] H. Pan, J. Li, and Y. P. Feng, "Carbon nanotubes for supercapacitor," Nanoscale Res Lett, vol. 5, pp. 654-668, January 2010.

[13] S. Hussain, R. Amade, E. Jover, and E. Bertran, "Nitrogen plasma functionalization of carbon nanotubes for supercapacitor applications" J Mater Sci, vol. 48, pp. 7620-7628, August 2013.

[14] J. Pérez, "Ultra-long VA-CNTs and CNT-MnO_2 composites for supercapacitor applications," M.S. thesis, Universitat de Barcelona, Barcelona, Spain, 2012.